Proceedings of the 3rd International Conference on Materials Chemistry and Environmental Engineering (CONF-MCEE 2023), Part II
DOI: 10.54254/2755-2721/7/20230499

Natural superhydrophobic surfaces and recent advances in synthetic superhydrophobic surfaces: A review

Yaojia Shen[1], Mingzhang Tang[2], Yinze Liu[3], Xirong Li[4*], Zhuoyou Li[5]

[1]Chengdu Foreign Language School, Cheng du, 610031, China
[2]Metropolitan Preparation Academy, Toronto, M3B 1Z2, Canada
[3]Hongwen School Qingdao Laoshan Campus, Qingdao, 266101, China
[4]Departemnt of Chemistry, University of Manchester, Manchester, M139PL, UK
[5]Chemical and materials engineering, University of Leeds, Leeds, LS29JK, UK

*1278685631@qq. com

Abstract: This review uses modern technologies to discuss the hydrophobicity mechanism of various natural surfaces found and studied in recent decades and their chemical components and delicate surface structure. It also contains many invent inspired by lifelike superhydrophobic characters, and tons of human living has been solved with the help of these applications. Also, the theories of how low hysteresis is induced by high contact angle devoted to the ability of water-repellent, drag reduction, and self-cleaning of a bunch of natural creatures are presented along with their characteristics. Besides, some of the recent fast, eco-friendly fabrication methods of superhydrophobic are discussed with the application of superhydrophobic surfaces in industry. Furthermore, the problems and challenges currently facing how to make the fabrication methods of the superhydrophobic characters better fit the industrial manufacture.

Keywords: superhydrophobic surface, fabrication methods, applications, difficulties, improvement

1. Introduction

In the long history of evolution, nature has fostered numerous astonishing creatures that live in wildly varied environments. To survive all the dangerous surrounding conditions, such as being submerged by water puddles, being infected by the spores of fungus in the air, or getting wet and killed by violent rain, many animals and plants have developed superhydrophobic surfaces that can repel water and can be self-cleaning. The superhydrophobicity of characters can be promoted in two ways. One uses low-enface energy materials or covers the origin surface with polytetrafluoroethylene, silicon, or wax. The other is creating high roughness conditions to increase the surface area.

On the contrary, if the roughness of a hydrophilic surface is increased, then the character would be more hydrophilic. Whether a surface is hydrophobic or not is defined by the contact angle when the value of the contact angle is lower than 90°. In contrast, if a contact angle is higher than 90°, the surface is proved to be hydrophobic.

The contact angle can be affected by roughness, surface cleanliness, or texture. Many models have been established to determine the impact of roughness on the contact angle. Wenzel set an equation that helps illustrate the revised contact angle when a surface's net energy decreases while droplets spread on

DOI: 10.54254/2755-2721/7/20230499

it. After several years, Cassie and Baxter consummate the Wenzel equation by extending the situation when there is an additional interface between liquid and air with air pockets remaining between valleys and bumps on the surface. This equation Illustrates shows how significant surface roughness is for its superhydrophobicity. It also allows researchers to design synthetic materials with the same property. By using scanning electron microscope (SEM) imaging and much other equipment, scientists have many micros and even the nanostructure of creatures that can repel water. In 1997, Neinhuis and Barthlott studied hundreds of different plant species, one of which in lotus leaf. Later, they found an inspiring quality that the lotus leaf has: the "lotus effect." Lotus leaf has such a high contact angle value and shocking self-cleaning properties regarding its hierarchical structure that leaves big air pockets and hydrophobic wax covering. What's more, rose leaf, being different from lotus leaf, can avoid being wet by having the droplets roll off once they come into contact with the leaf. The structure with bumps with ridge surrounding of colocasia leaf provides an excellent capability to bind water back. Not only do plants have such a peculiar water-repellent surface, but similarly, animals have diverse methods to avoid being wetted by water too. The superhydrophobic surface of the springtail enables it to avoid being submerged when water droplets hit on it. Water striders can walk on water surfaces with the help of their unique body structure, which enables them to capture prays and survive. The butterfly wing is capable of shedding water off at a specific angle in a particular angle due to its anisotropic wettability and scales on it. Many models can be produced by replicating all these various structures to imitate the surface hydrophobicity and self-cleaning properties. Applying these properties to military, domestic, agricultural, and many other biomimetic-inspired industries, these surfaces can save significant human and economic resources on waterproof, fog proof, snowproof, corrosion resistance, and anti-fouling fields. In this article, to fit our goal of using new material technology for social contribution, many eco-friendly and inexpensive fabrication of superhydrophobic surfaces in laboratories created in recent years will be discussed. Also, the basic principle of natural superhydrophobic surfaces will also be addressed [1,2].

2. Theory

2.1. Surface tension and surface classification

Surface tension is the cohesive force exhibited by liquid molecules that allow the surface of a liquid to resist an external pressure exerted on it to some extent. They attract other molecules nearby that are stronger than those underneath the surface, creating surface tension. A liquid feels like a thin film that tends to maintain its integrity, so the water droplet forms. This force also causes air to bubble up in the liquid. When molecules on the surface of a liquid pull other molecules on the surface, the liquid forms a sphere. The tangent line of the sphere contacts the surface, and the cover itself includes an angle between the solid, liquid, and gas phases. The angle created is defined as the contact angle, and we can use this to classify the properties of different surfaces.

2.2. Surface energy

The molecules on the surface of any matter have less bonding or attraction between themselves and other molecules beneath the surface. But on the other hand, these molecules have higher free energy so that they can form new bonds with other contact surface molecules. The free energy here is called surface energy, measured in J/m2 or N/m, which can be presented as energy per area or force per linear distance on the surface. It can be modeled as the equation.

$$WSL = \gamma_{SA} + \gamma_{LA} - \gamma_{SL}$$

where WSL is the work of adhesion per unit area, γ_{SA}, γ_{SL}, and γ_{LA} are the solid-air, solid-liquid, and liquid-air surface tensions, respectively. [1]

2.3. Young's model and equation

Young's model is the fundamental model for studying the wetting properties of the surface. Apply to the figure [Figure. 1-c], the young's contact angle is measured in θ0. It determines the non-wetting property

DOI: 10.54254/2755-2721/7/20230499

of the character. As shown above, when θ0 is less than 10°, the surface is super hydrophilic; then, as θ0 between 10° and 90°, the surface is defined as hydrophilic. The hydrophobic surface appears if θ0 lies between 90° and 150°. While θ0 is more significant than 150° with low hysteresis, a superhydrophobic character emerges. With the surface tensions mentioned in 3.1, scientists can calculate young's contact angle through young's equation:

$$cos\theta_0 = \frac{\gamma_{SA} - \gamma_{SL}}{\gamma_{LA}}$$

Besides, not all the non-wetting surfaces are smooth. To measure the apparent contact angle on a rough surface [Figure. 1-d], scientists define another equation to solve:

$$cos\theta_{obs} = r * cos\theta_o$$

Where θo represents the young's contact angle on the smooth surface, and r is the roughness of the surface that is calculated by dividing the actual surface area A_{SL} of the surface by the projected surface area A_F, which is：

$$r = \frac{A_{SL}}{A_F}$$

Since the roughness of the rough surface is always not less than 1, the θobs will cost less than θo when θo is less than 90°, but θobs will be greater than θo when θo is greater than 90°. This makes hydrophilic surfaces more hydrophilic and hydrophobic surfaces more hydrophobic. [2]

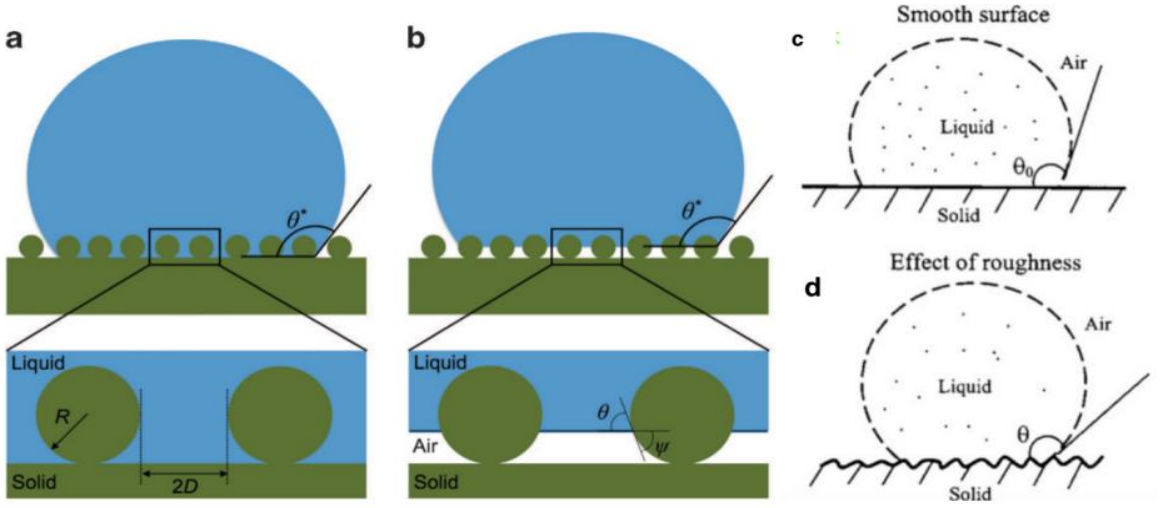

Figure 1. Schematic of a liquid droplet in contact with different kinds of surfaces in other states that water contacts. a) Water contacts in Wenzel state, b) Cassie-Baxter state. [2]. c) Young's contact model on a smooth surface, d) Young's contact model on a rough surface [1]

2.4. Wenzel & Cassie-Baxter model

While young's model illustrates the basic things about the contact angle, scientists also summarize the calculation result of the overall free energy of superhydrophobic surfaces and classify them into two main models: the Wenzel state and Cassie-Baxter state. In the Wenzel State, the gap between peaks on the surface is filled with water while the water droplet contacts the surface [Figure. One a)] so the interphase between solid and liquid is thoroughly wetted, and scientists could determine the apparent contact angle by using the Wenzel equation:

$$cos\theta obs = r * cos\theta o.$$

Here θo refers to the young's contact angle. However, since the roughness is always greater or equal to 1, those liquids with low surface tension, like hexadecane and other oils, still maintain a soft contact angle in the Wenzel state.

On the other hand, if the space between bulges does not fill with liquid, the model is in the Cassie-Baxter state [Figure. 1 b]. Since the existence of the air pocket, the liquid does not completely wet the

DOI: 10.54254/2755-2721/7/20230499

surface. To figure out the apparent contact angle, research uses f_{SL} to determine the fraction of the interphase between solid and liquid, and the formula calculates it

$$f_{SL} = r_{\varphi} * \varphi_s.$$

Where r_{φ} is defined as the roughness of the area that the interphase of solid and liquid locates, and φ_s is the area fraction of the projected liquid–air interface occluded by the surface texture. Then they get an equation of how they calculate the observed contact angle:

$$cos\theta obs = f_{SL} * cos\theta + f_{LV} * cos\pi = f_{SL}\, cos\theta_{O} - f_{LV}.$$

They also claim that this equation gives liquid to form a higher contact angle compared to the Wenzel state, although the contact angle is less than 90°. In addition, because of the air buckets between bulges, the solid-liquid fraction f_{SL} is much lower than the Wenzel state. This gives a low hysteresis ($\Delta\theta$) for liquid even though it has low surface tension. [2]

3. Classical Natural Superhydrophobic surfaces

3.1. Plants

3.1.1. Lotus leaf. The first strategy is that the leaf surface achieves high roughness via hierarchical structure due to the papillose epidermal cells. Second, the wax covering the leaves, composed of long-chain hydrocarbons [3], is relatively hydrophobic. The combination of the two influential factors makes the non-wetting properties of a lotus leaf. [Figure.2]

Since the roughness closely correlates with the contact angle, we may change the roughness to influence the contact angle. [Figure.3a] shows a group of the contact angle values when the leaf is original, uncovered of wax, covered with paraffin wax, and flattened via calculation. The fresh leaf's contact angle is approximately 126° [4]. In comparison, it is reported that the contact angle of a water droplet against the paraffin wax is 104° by Craig et al. and Kamusewitz et al. [5&6]. Moreover, the flat leaf is estimated at 76° for the contact angle [4]. [Table 1.] shows the contact angles after the wax dissolution of 2 hydrophilic plant surfaces — Fogus and magnolia and another hydrophilic plant surface— colocasia. The hydrophilic plants without an original wax covering are barely affected [7]. It is assumed from these two figures that both the bumps and the resin are crucial for the lotus leaf's hydrophobicity. Moreover, the thin wax layer grows by crystallization and self-assembly in a spatial orientation that is vertical to the cuticle of epidermal cells, which increases the surface roughness even more [3]. Furthermore, the contact angle decreases if we dry out the leaf so that the bumps' height decreases along with the shrinkage. From that point, as the spots on surfaece reach their maximum height, the contact angle gets to its maximum.[7] [Figure.3b]

Additionally, there are two techniques for us to take a deeper look into the surface structure: an optical profiler and an AFM scan. Since AFM cannot conventionally measure the height of bumps of the lotus leaf when it's fresh, it is accessible to take two scans from the top and the bottom, respectively, and fuse the images. Associating the data from the two instruments, more details of bumps are observed. Table.1 compares the P-V distances (peak-to-valley distance), mid-width, and peak radius of micropumps and nano bumps of lotus leaf and other plants' leaves. It is easy to see that with the high P-V distance and small peak radius the lotus leaf has, it becomes hydrophobic since it has a higher roughness. Besides, the hierarchical structure combines microscale and nanoscale and is likely more hydrophobic than the two scales solely [7].

DOI: 10.54254/2755-2721/7/20230499

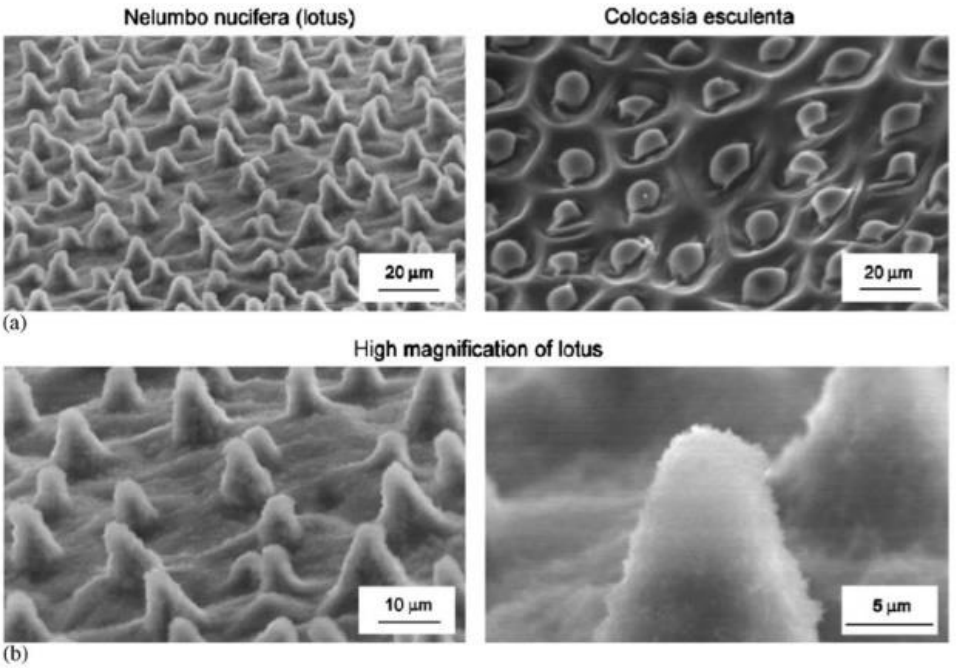

Figure 2. (a) SEM imaged Lotus and colocasia leaf surface structure. (b) Two high-magnification SEM images contain the more detailed design of the lotus leaf. (Adapted from Burton, Z., & Bhushan, B. 2006) [4]

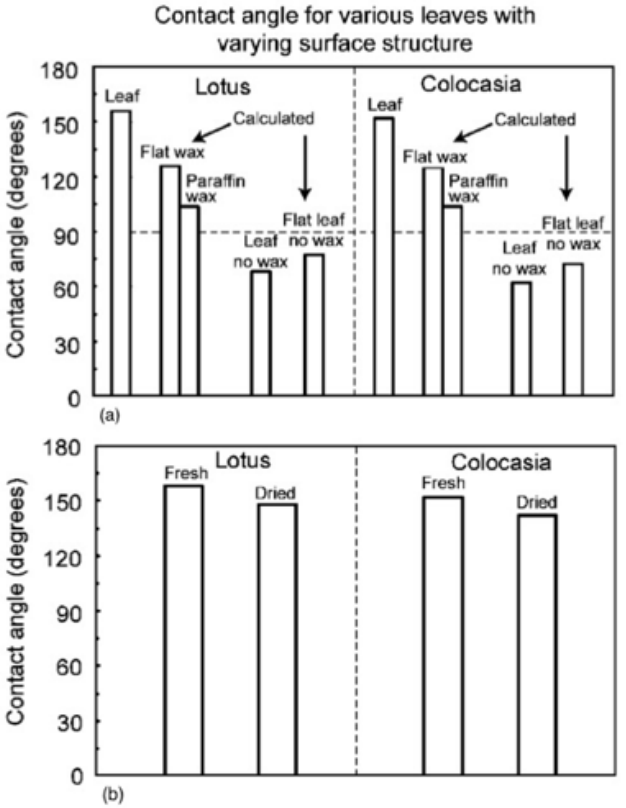

Figure 3. Contact angle calculations and measurements for original and flat leaf surfaces of both fresh and dried leaf. (Adapted from Burton, Z., &Bhushan, B. 2006) [4]

DOI: 10.54254/2755-2721/7/20230499

Table 1. Statistics of micropumps and nano bumps of both hydrophilic and hydrophobic leaves when they are fresh and dry, using AFM and an optical profiler. [4]

		Micropump (μm)				Nanobump (μm)		
		Scan size (50 μm × 50 μm)				Scan size (2 μm × 2 μm)		
Leaf		P-V height	Mid-width	Peak radius		P-V height	Mid-width	Peak radius
Lotus								
Fresh		13[a]	10[a]	3[a]		0.78[b]	0.40[b]	0.15[b]
Dried		9[b]	10[b]	4[b]		0.67[b]	0.25[b]	0.10[b]
Colocasia								
Fresh	Bump	9[a]	15[a]	5[a]		0.53[b]	0.25[b]	0.07[b]
	Ridge	8[a]	7[a]	4[a]		0.68[b]	0.30[b]	0.12[b]
Dried	Bump	5[b]	15[b]	7[b]		0.48[b]	0.20[b]	0.06[b]
	Ridge	4[b]	8[b]	4[b]		0.57[b]	0.25[b]	0.11[b]
Fagus								
Fresh		5[a]	10[a]	15[a]		0.18[b]	0.04[b]	0.01[b]
		4[b]	5[b]	10[b]				
Magnolia								
Fresh		4[a]	13[a]	17[a]		0.07[b]	0.05[b]	0.04[b]
		3[b]	12[b]	15[b]				
[a] Data measured using an optical profiler.								
[b] Data measured using AFM.								

3.1.2. rose petals. In addition, apart from lotus leaves, rose petals also display high contact angles. From the physical structure, the wax shape of the cuticle of rose petals is one of the main reasons for its superhydrophobic properties. The layered surface of rose petals enables water droplets to be strongly adsorbed even at large observed contact angles. Its surface has wax crystals, which can be divided into three small parts: platelets, rods, and tubes. The plates are flat, thin, and attached to the rose petals' bottom layer. They can be round with top edges, or they can be irregular. Tubules are similar to rods in size and length, and as the name suggests, their shape looks like hollow cylinders. The wax on the rose petals consists mainly of a mixture of long-chain fatty compounds, mostly nonacosanol and nonacosanediols. The resin is hydrophobic and has a contact angle of approximately 95- 110º degrees with water. Moreover, another physical property of rose petals is their hierarchical structure, a feature shared by many plants with superhydrophobic surfaces. [8]

The hierarchical surface structure of rose petals makes water droplets adhere firmly even at large observed contact angles. The water droplets can stick firmly to the surface of the rose petals, which significantly increases the contact area between solid and liquid. Cassie-impregnated or Wenzel state droplets penetrate the spaces between surface features, resulting in higher adhesion to the rose. Like lotus leaves, there are microscale mastoids on the surface of rose petals, but they are slightly wider. Rose petals are confined mainly to the upper region of the mastoid process. As a result, water is more likely to penetrate between the microscopic structures on the petal surface. [9]

To study the wettability of roses, Chakraborty et al. experimented [10]by gluing petals on a glass slide with double-sided tape and then placing it on a goniometer to measure the apparent static contact angles at six different positions of the petals. The mean value of measured contact angles was 151º. The advancing and receding contact angles were measured by the standard fixed drop method, indicating the hysteresis of the contact angles. Then, an SEM was used to evaluate the petal surface structure, as shown in Figure.2. [10] The rose petal was also scanned with a high-resolution 3D confocal microscope to accurately visualize the liquid-air interface's position. The self-fluorescence properties of rose petals were used to label the surface while adding low dye concentrations to water helped imagine the liquid phase. Cross-sectional images obtained by confocal scanning showed clear evidence of a liquid-air

DOI: 10.54254/2755-2721/7/20230499

interface on the contact surface of the droplets, confirming that the liquid was only partially wetting the gaps between the tiny nipples. This conclusion contradicts the common assumption about the Cassie impregnation wetting state of rose petals. [10] According to the comparison between model prediction and experiment, it is determined that water has Cassie Baxter characteristics. The macroscopic wetting characteristics of roses are attributed to the composite Cassie--Baxter wetting [10]

3.2. Animals

3.2.1. Water Strider. Talking about animals that have superhydrophobic surfaces, one famous example is a water strider. Water striders have super long, nonwetting legs that enable them to stand freely and move quickly on the water without sinking. One of the important reasons for its superhydrophobicity is the nano-texture of its skin surface. These nano textures can reduce the adhesion force generated on the surface, convert the surface energy into kinetic energy, and make the droplets slide down. Water striders living in highly humid environments have cone-shaped setae on their legs. In the absence of any external force, tiny droplets of condensation slip off the legs of a water strider due to the presence of bristles. [11]

3.2.2. Springtail. Springtail (*Collembola*) owns another kind of non-wetting property. Since their habitat is deep into the soil and water polluted by organic chemicals, they have evolved their superhydrophobic cuticle to protect themselves against these contaminants.

Researchers obtained a clear image of the surface structure using SEM and TEM. It shows a bristle in the micrometer size [Figure 4], similar to the water strider. And the surface morphologies of the cuticular structure of the springtail (*Tetrodontophora bielanensis*) are shown in Figure [4]b, where mushroom-like reentrant structures are illustrated. As shown in [Figure.5]b,c, the concave top shape of the overhanging features is also a critical factor for the solid, liquid repellency of the springtail [13], which allows the springtail to maintain a high advancing angle with water about 152.9 degrees. When the water droplet contacts its tail, this value can reach 165 degrees. [Figure 6]

By using Sum Frequency Generation (SFG) Spectroscopy, scientists proved the existence of the wax coat on the surface [13], and it helps the organism to maintain its non-wetting properties [13].

Figure 4. SEM image of the cuticle of O. cincta (*Collembola*, Entomobryidae) [12]

DOI: 10.54254/2755-2721/7/20230499

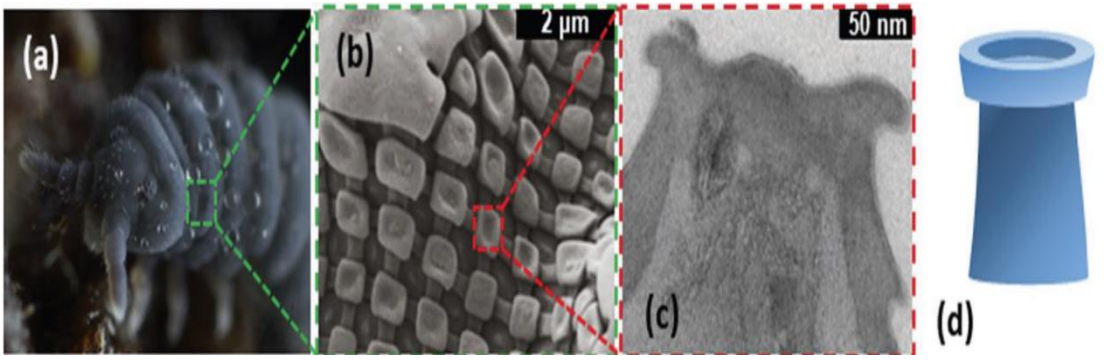

Figure 5. a) Photograph (courtesy of Brian Valentine). b) SEM image and b) TEM image c) of a springtail, *Tetrodontophora bielanensis* (*Collembola*, Hexapoda), with omniphobic cuticular structure. [13]

3.2.3. Butterfly Wings. As another example of a hydrophobic surface, the butterfly wing is unique since it has anisotropic as well. Anisotropism is a property that, as water droplets fall on butterfly wings, they will fall off more efficiently when the wings incline at certain angles [14]. The flexible ridges and veins take effect in this leading direction [15]. Likewise, this property closely correlates the wings' micro-scale, submicron-scale, and nano-scale structures, contributing to their hydrophobicity.

The structural characteristics and chemical components of butterfly wings have been studied by Steve Hermann [16]. The wings are covered by scales that are organized like overlapping tiles. Depending on their shapes, the scales can be divided into three groups: angustifoliate, latifoliate, and round-leaved [17]. On the one hand, the micro-class scales with 48-91 um gaps between them are composed of submicron vertical gibbosities and horizontal links on their surface. The cross sections of gibbosities are regular triangles and are in a parallel, joint arrangement [Figure. 6]. On the surface of the gibbosities, there are nano protuberances. [Figure.7] These complicated structures give the wings a high water-repellent ability to fly on rainy days. In Fang et al.'s experiments [18], they set three different mathematical models to figure out the utility of every structure. As a result, without the other structure, the wing with scales only or with gibbosities cannot reach its original contact angle. Also, compared with the wing without scales, the wing's contact angle gets promoted by 14.3° - 43.3°. The two experiments claim how the peculiar structure contributes to the surface's high contact angle [18].

Finally, the chemical component of butterfly wings is also of great importance. The wings have a Chitin cover, a hydrophobic material with a contact angle of around 100° [18]. The alternation between chitin and air on scales allows air pockets to be sustained if water droplets fall on the wings [15].

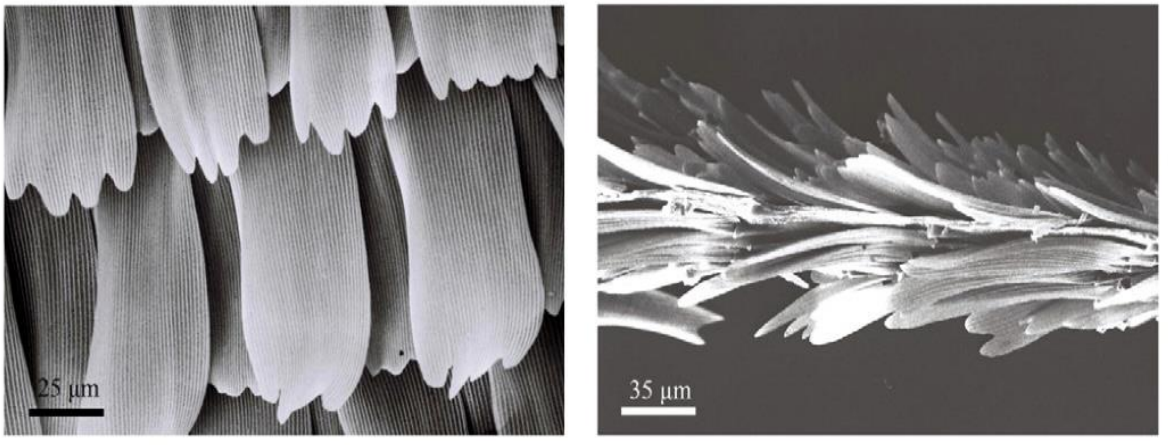

Figure 6.SEM images of butterfly wing’s structure. [14]

DOI: 10.54254/2755-2721/7/20230499

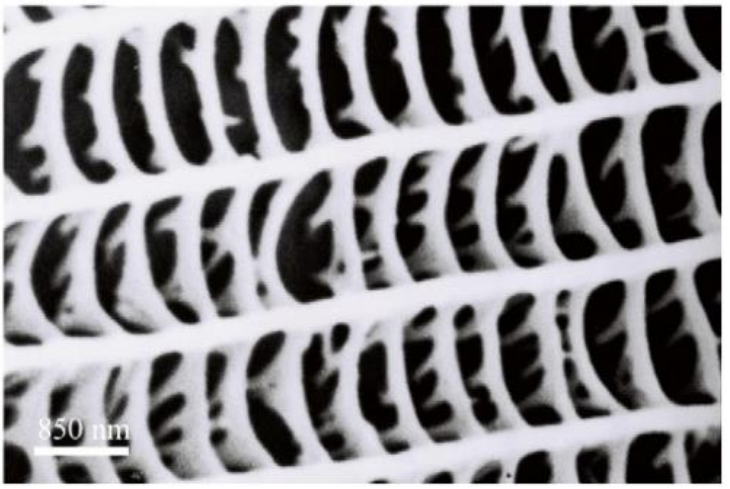

Figure 7. Gibbosities And horizontal links on the scale. [14]

4. Other natural superhydrophobic surfaces

4.1. Shark Skin

Shark skin is a hydrophobic material. Because of its extraordinary ability in drag reduction, it can also be used to fabricate hydrophobic materials for use in underwater activities and sports. The mucus on the skin of sharks and the ribbed texture is worth discussing to find out the secret behind its properties [19].

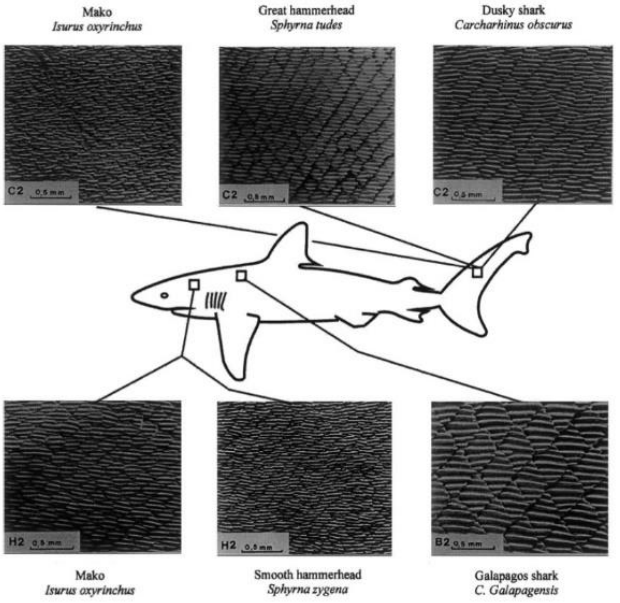

Figure 8. Scale patterns of different kinds of fast sharks. (Adapted from Reif, W. E. 1985) [21]

Every kind of fast-swimming shark has different shapes of riblet-topped scales aligning towards the direction of water flow with different spacing between, and even other body parts of a shark are characterized by their unique scale shapes in great diversity [20, 21]. Figure.8 shows the various scale patterns from a single fast-swimming shark specimen. Due to their sharp edge and unique forms, the scales are called dermal denticles (skin teeth). The interlocking scales resemble tiny riblets, reducing up to 9.9% of the drags produced by the shark's movements [22]. The creatures must overcome various pressure and drags to swim faster in the fluid. The most important two are pressure drag and friction

DOI: 10.54254/2755-2721/7/20230499

drag, which are assumed to be the friction pull between adjacent molecules in the same fluid direction. Pressure drag is easily reduced by having a streamlined shape since it is the pressure produced by moving water around the creature's surface. Friction or viscous drag is created by interacting with surface molecules. As the fluid becomes thicker, its breath on the animal rises [19]. The viscous sublayer is the most organized in the fully developed turbulent flow. At the same time, the layer closest to the touched surface is more chaotic and disorganized, affected by the outer bursting vortices in streams.[23] These diverse flows are sharks' leading cause of drag, meaning they need extra energy to compensate for the lost momentum transfer. And the impeding riblets are essential to reduce such a drag. Although the mechanism is yet not entirely understood, some experiments have revealed much of its effects. One particular function the riblets have is that they increase the wetted area. The tips cause to contribute to high-velocity flow in smaller content. In contrast, the valleys causing low-velocity flow contribute to low-shear stresses and the rare occurrence of vortex ejection [24]. The sharks swim faster with high momentum transfer and lower drag [19].

From the aspect of chemical composition, the sharks are covered by mucus on the skin. A natural polymer the fish secreted can reduce the drag by up to two-thirds [25]. Together with the spacing between the scales, the mucus stops microscopic aquatic organisms from adhering and brings friction between its body surface and surrounding objects [26].

4.2. Gecko's Feet

Gecko's feet have attracted considerable attention in material science since they can adhere to the wall vertically. However, the skin of geckos has received relatively little focus. As most species of geckos live in a semi-arid climate and the surrounding environment is composed of various contaminants from solid, liquid, and air [27], the skin of geckos gives them plenty of properties that enable them to survive. These include hydrophobic, self-cleaning, and radiation reflection [28, 29]. The hydrophobicity of the gecko's skin will be explained and discussed in the following paragraphs.

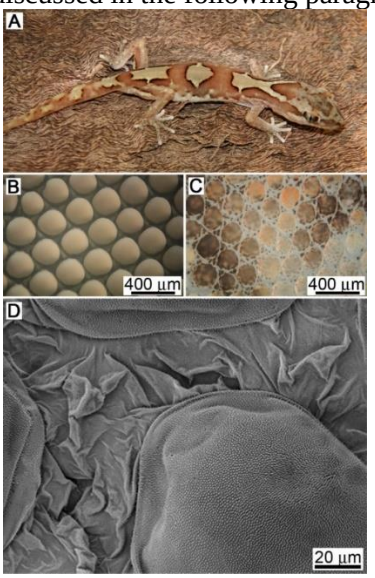

Figure 9. (A) Photo of a kind gecko called *Lucasium steindachneri*. (B) Optical image of the microstructure of the outer skin on the abdomen region and (C) dorsal region of a gecko. (D) SEM image of scales on dome region and areas between lizard scales. (Adapted from Watson, G. S., et al. 2015) [27]

The micro and nanostructure are visible if we take specimens of the gecko's skin and take optical images of them from the abdomen and dorsal region. (Figure.9) These regions consist of dome-shaped scales; abdominal scales are more significant than dorsal scales, with larger spacing between scales [27]. On the surface of the scales, there are spinules(hairs) with sub-micron spacing, the majority of which are capped with some curvature on the top. (Figure.10) From a previous study, we can figure out that the Oberhausen (thin outer layer) of the skin is primarily keratin for most gecko species [30, 31]. These

DOI: 10.54254/2755-2721/7/20230499

scale and hair structures and the thin layer covering the surface are the principal reasons the gecko's skin has such a high hydrophobicity. The contact angle of skin in contact with water is measured within the limits of 151-155°, demonstrating that this surface is superhydrophobic [27]. Moreover, the gecko's skin also has a low hysteresis comparable to a lotus leaf, so droplets are difficult to stay stable instead of rolling off. That's the reason why the skin can self-cleaning [27]. The droplets can still establish a high contact angle even if we conform the skin to a flat form. In experiments by Watson et al., whether the droplets were large or small or from different liquids, they would all bounce back after contacting the gecko's skin surface [27].

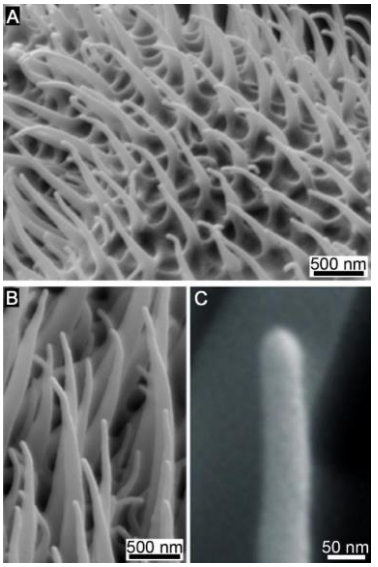

Figure 10. SEM images of the microstructure on the dorsal gecko scale. (Adapted from Watson, G. S., et al. 2015) [27]

5. Fabrication method of bionic material in the laboratory

Superhydrophobic surfaces are significant in fundamental science and have broad industrial applications, leading to people conducting further research on their fabrication methods.

The superhydrophobic surfaces can be used for

· Oil-water separation,
· Anti-icing,
· Self-cleaning,
· Corrosion resistance,
· Drag reduction,
· Solar cells,
· Bio-medical,
· Antifouling technologies, etc.

Also, many fabrication methods have been proposed, including immersion, electrospinning, electrodeposition, plasma etching, layer self-assembly, and chemical vapor deposition. However, for the fabrication methods to fit practical use, they should first be eco-friendly to reduce the pollution and contaminants made during the fabrication. Second, it requires the process to be fast to minimize the fabrication duration and cost. In addition, the superhydrophobic surface should possess a larger water contact angle, mechanical durability, and chemical stability. Lastly, inexpensive fabrication can better fit the actual industrial applications.

This part mainly focuses on fabrication methods of superhydrophobic surfaces, which are eco-friendly, rapid, inexpensive, and able to produce excellent products.

5.1. Preparation of superhydrophobic surfaces by atmospheric pressure plasma

The plasma treatment method is a modern superhydrophobic silicone rubber surface technology. This treatment requires a Design of Experiments (DoE) by setting the parameters of different plasmas; the magnitude of the wetting behavior on the substrate will vary. [32]

The object of choice for this experiment is silicone rubber, a polymer-based insulator. Silicone rubber

DOI: 10.54254/2755-2721/7/20230499

was chosen because it has low surface energy. However, the waterproof performance of silicone rubber has not reached a satisfactory level, so the surface of the silicone rubber needs to be changed to achieve good waterproof performance.
The experimental method used in this paper is an atmospheric pressure plasma jet. It impacts the surface to be treated through a nozzle, thereby changing the surface energy. [32]

This paper adopts the practical design method for the specific experimental design and procedures. It selects the design factors for the water contact angle (CA) and the contact angle hysteresis (CAH). From the results of the experimental parameters in table1, when the power reaches the maximum capacity and the distance between the nozzle and the substrate is the smallest, the size of CA is 155.1°, and the size of CAH is 1.6° [32]

The experimental conclusion is that preparing a superhydrophobic silicone rubber surface by atmospheric plasma is a modern method that has attracted much attention, which is efficient, low-cost, and pollution-free.

5.2. Fabrication of superhydrophobic surface on stainless steel by two-step chemical etching

The use of two-step chemical etching is a technology that has been modernized in the last two years, and it has two main advantages. The first is that it does not require costly equipment, and the processing procedure is relatively simple and only needs hydrochloric acid and ferric chloride. This two-step chemical etching method requires hydrochloric acid and ferric chloride, adding stainless steel to Add hydrochloric acid first and add ferric chloride after the hydrochloric acid is etched. The micro- and nanostructures produced on the surface are modified with fluor silane. Finally, a contact angle (CA) of 159° and a contact angle hysteresis (CAH) of 2° [33] were obtained by measurement. In the experiment, by adding different etching parameters, it is judged that the best etching parameters have the most significant impact on the surface of stainless steel.

The first is that the etching parameters involved in immersing the stainless-steel surface in hydrochloric acid have two aspects: the concentration of hydrochloric acid and the etching time. When the concentration of hydrochloric acid increases, the hydrophobicity of the stainless-steel surface will first increase and then decrease. The growth is because the addition of hydrochloric acid concentration will cause the roughness and contact angle of the stainless-steel surface to rise. The decrease is because the concentration of hydrochloric acid increases to the point where excessive corrosion occurs on the surface. In terms of etching time, it was concluded through experiments that the hydrophobicity increases with the rise of etching time. The resulting CAs were finally measured to be 159° and 2° of contact angle hysteresis. [33]

Then the stainless-steel surface is immersed in $FeCl_3$, and the etching parameters involved in this process are the etching temperature (X) and etching time (Y). When $0<x<100$, the wettability of the stainless-steel surface is low. When $x=100$, the wettability of the stainless-steel surface is excellent, and the contact angle is 159°. When $x>100$, the surface will accelerate corrosion due to high temperature. In terms of etching time, when the etching time is 4 hours, the wettability of the stainless-steel surface is the highest. [33]

5.3. Fabrication of superhydrophobic surface on low-carbon steel

Low-carbon steel is widely used in the automotive or aviation industries because of its good ductility and corrosion resistance. But one of the shortcomings is that the hydrophobicity of low-carbon steel is not very good, so some treatment methods are needed to prepare a better hydrophobic surface. [34] The method of laser surface treatment is adopted in this paper. The principle of laser surface treatment is first to use a laser to treat the surface of the mild steel until a circular texture is formed, then use a laser marking machine to process the mild steel with a circular texture, and add wax and candle smoke, respectively. Finally, the hydrophobic angle of the soft steel surface was changed from 87° to 155°. [34] The experimental method is to process the diameter and spacing of the surface of the mild steel by laser to achieve the formation of circular texture on the surface and then use the laser marking machine to process the circular texture on the surface of the mild steel, and finally, smear the surface of the sample. Wax is heated to a specific temperature and then smoked with candles for deposition.

Experimental Conclusion In this paper, the preparation of the superhydrophobic surface of low

DOI: 10.54254/2755-2721/7/20230499

carbon steel is completed by laser surface treatment, the roughness of the surface of low carbon steel is changed by laser, and then the circular texture is processed by laser marking machine to make the surrounding surface produce Cylinders, for better deposition of candle smoke (soot particles with low surface energy) below. Finally, the whole experiment was completed, and it was found that the contact angle number of the mild steel changed from 87° to 155°. In general, the roughness of the object's surface and the change in surface energy will affect the hydrophobic performance of the thing. [34]

5.4. Laser Texturing Method

Metals are used daily in construction, vehicle manufacturing, and other industries. However, most metals do have some problems that make them cannot be long term use, including corrosion and fouling. Also, ice accretion happens on power cables, wind turbines, and aircraft wings. [35] However, superhydrophobic surfaces can essentially prevent these issues by increasing the corrosion resistance [36], antifouling ability [37], and anti-icing ability [38]. The fabrication methods to impart superhydrophobicity to metal substrates include electrodeposition, topography transfer, chemical etching, lithography, and sol-gel processing. Laser texturing is a popular method for superhydrophobic surface structure fabrication [39]. The advantages of this technology include high-precision patterning, reproducibility, low process cost, fast process speed, and low contamination, which makes this technic very suitable for industrial superhydrophobic surface fabrication. [39]

The metal oxide formed during laser texturing makes the surface super hydrophilic with high surface energy. The wettability of the laser-textured metal surface transit from superhydrophilic to superhydrophobic by exposing it to ambient air. However, this transition process usually takes an extended period. The post-process with silicone oil heat treatment for robust superhydrophobic stainless steel surfaces was developed to make this a rapid method to fit actual industrial applications better. A nanosecond pulse laser was used to construct the micro and nanostructures on titanium, aluminum, and copper with an ultrafast, simple, and eco-friendly post process in 10 min of silicone oil heat treatment, which can give the metals superhydrophobic surfaces.[39] The characters can pass stability and durability tests, including sandpaper abrasion, knife scratches, use of a buffer solution, aging tests, and especially its facile repairability, which shows its potential for industrial applications and a wide range of services.

5.5. Anodization and aqueous acid treatment

The superhydrophobic surface fabrication methods have been improved mainly in the past decade, and the potential of it and its widespread uses led to further research on how to make the process faster and cheaper—also, some focusing more on improving durability and stability.

Inspired by lotus leaves, advanced research on the superhydrophobic surface with good self-cleaning was carried on.[40]

Research in 2019 focused on preparing superhydrophobic titanium surfaces by single-step anodization in the organic electrolyte. The stearic acid modification comes right after, wherein the titanium surface can be anodized to form micro-nano hierarchical morphology. The anodized titanium is treated with stearic acid to lower the surface energy and make the surface superhydrophobic.[41] By changing the anodizing parameters like time of the process and voltage, an optimized result of the contact angle around 160.1°± 0.5˚ was given under 35v and 3 hours.[41] The stability of titanium with a superhydrophobic surface was tested by 48h immersion in aqueous solutions of different pHs (pH=1 and pH =13) and turned out with good stability and durability in acidic solutions. The self-cleaning ability was also tested by adding droplets on the surface set in an inclined position of 5° to 10°. The droplet can roll off easily on the contamination instead of sticking on the surface, like the phenomenon of droplets on bare titanium. The results turned out that the superhydrophobic surface with excellent self-cleaning performance.[41]

Though the results gave an excellent superhydrophobic surface with exceptional quality, the duration of the process was way longer than other fast processes.

Another research in 2020 focusing on self-cleaning also used anodization in the fabrication process of superhydrophobic surfaces on titanium. The durable superhydrophobic titanium surface was created through simultaneous anodization and adsorption of a myristic acid mixture. The anodization potential,

DOI: 10.54254/2755-2721/7/20230499

acidic concentration, and length of time for anodization can also optimize the performance of the coating. The optimized result with a contact angle around 174.4 ± 1.2° made under 50v anodization potential, 2mins duration, and the volume ratio of myristic acid solution to HCl of 50:3.[42] It gave out an excellent self-cleaning property to the surface, which was tested using graphite powder of mesh size around 150μm and myristic acid as contaminants. The experiment was carried out when the character inclined at 8° and showed an excellent self-clean ability. In addition, the stability test was done under acidic, neutral, and basic environments and the mechanical durability was tested by scratch for a certain distance on grit SIC paper. Gave out a similar result compared with the previous research; the surface has suitable self-clean properties and excellent chemical stability in acidic environments. It is worth mentioning that the contact angle can stay above 150° even with the abrasion distance approaching 300mm. [42]

6. Application

6.1. Anti-icing

Icephobicity is one of the directions in that superhydrophobic surfaces develop. For the superhydrophobic characters, scientists mainly focus on the ice adhesion strength on superhydrophobic surfaces. The past literature illustrates that the superhydrophobic with nanostructure cannot experience oleophobicity since the Cassies-Baxter state will break when water freezes at supercooled airflow conditions. Therefore, the researchers focus on flat superhydrophobic surfaces, and the result shows that the flat superhydrophobic surfaces have a better oleophobicity than the nanostructure one [43]. But on the other hand, since the ice adhesion strength will actually increase, so the application of superhydrophobic surfaces in the anti-icing process is limited [44]. So far, these surfaces are used in different places like the aircraft wings, the ship's hull, the inner wall of the refrigerator, and so on.

6.2. Antibiofouling

In the aquatic environment, the ship's surface has to face the situation that some organisms, like bacteria, may stay on the surface. They will decrease the boat's speed since they destroy the structure of the boat's surface, and the stress on the engine and fuel consumption will also increase [43]. Some researchers try to use non-wetting properties to resist the adhesion of this aquatic life [45]. Among these superhydrophobic surfaces, the surface with the Cassie-Baxter state maintains the best anti-biofouling resistance because the liquid in the Cassie-Baxter state has a low fraction of touching to solid. The air bubble between liquid and concrete acts as a good insulator for bacteria to attach and cover all the areas of superhydrophobic surfaces. But on the other hand, since the Cassie-Baxter state is not stable, the liquid may change to the Wenzel state later after Cassie-Baxter. This gives a chance for the bacteria to attach to the surface. Also, the superhydrophobic surface is not smooth, and the adhesion of bacteria in the area is very high. [46] Until now, scientists are still trying to fabricate the covers with a stable Cassie-Baxter state when it is placed into a solution.

6.3. Anti-fogging

Because of the non-wetting properties of superhydrophobic surfaces, anti-fogging becomes one central direction of the development of the application of superhydrophobic surfaces. According to the observations in the laboratory, the water vapor liquefies into tiny droplets on the surface because of its high contact angle. Since the evaporation, they disappear quickly in 10 seconds. Compared to the superhydrophobic and glass surfaces, superhydrophobic surfaces show better properties in the anti-fogging process. It is used to make coatings on glasses, self-cleaning windows of tall buildings, solar cells glass panels, automobile rearview mirrors, and so on. [47]

7. Problems and Challenges & Future Outlook

The technology of fabricating excellent superhydrophobic surfaces has been improved mainly in the past twenty years. However, it is still a challenge to ensure the robustness and surface fragility of the products under extreme conditions. Take an example of the environment at a depth of 10m underwater, the hydrostatic pressure can quickly destabilize the surface conditions, and this transition is non-

reversible. Besides, the robustness of these materials is also a big problem for applications like PV and self-cleaning windows, as the products tend to degrade and erode over a period. [48] Furthermore, the degradation of superhydrophobic material is due to the accumulation of dirt when exposed to air for a long time.[49]

To solve these problems, further investigation on methods of enhancing robustness is necessary for the superhydrophobic surface to better fit practical use.

The mechanical durability of superhydrophobic surfaces can be another big problem as the microscale and nanoscale structures are susceptible to mechanical stresses. The cover can be damaged by rain, dust, aging, and decay. Passive regeneration and active repairing methods are used to solve the problems and make the surfaces fit daily use better. [50]

In addition, most research is done on flat and rigid substrate materials like metal surfaces and silicon wafers. Meanwhile, these fabrication methods reported in the literature always tend to be expensive or only applicable for small flat surfaces, and these methods are not suitable for large-scale production. To better fit daily use, the research should be directed toward large-scale fabrication methods with less expensive costs and in a more environmentally friendly way.

Though many problems and challenges have not been overcome, the potential of superhydrophobic surfaces has been proved by various applications like oil/water separation, self-cleaning, anti-fogging, anti-corrosion, anti-biofouling, ice phobic, which keep pushing the technology advances and contributing a better life for human beings. [44]

Acknowledgment

Yaojia Shen, Mingzhang Tang,Yinze Liu,Xirong Li and Zhuoyou Li contributed equally to this work and should be considered co-first authors.

Reference

[1] B. Bhushan, Biomimetics, Biological and Medical Physics, Biomedical Engineering, DOI 10.1007/978-3-319-28284-8_3

[2] Kota, A. K., Kwon, G., & Tuteja, A. (2014). The design and applications of superomniphobic surfaces. NPG Asia Materials, 6(7), e109-e109.

[3] Koch, Dommisse, & Barthlott. (2006). Chemistry and crystal growth of plant wax tubules of lotus (nelumbo nucifera) and nasturtium (tropaeolum majus) leaves on technical substrates. CRYST GROWTH DES, 2006,6(11)(-), 2571-2578.

[4] Burton, Z. , & Bhushan, B. . (2006). Surface characterization and adhesion and friction properties of hydrophobic leaf surfaces. Ultramicroscopy, 106(8-9), 709-719.

[5] Craing, R. . (1960). Physical factors related to denture retention. Journal of Prosthetic Dentistry, 10(3), 459-467.

[6] Paul, H. . (1999). The relation between young's equilibrium contact angle and the hysteresis on rough paraffin wax surfaces. Colloids and Surfaces A: Physicochemical and Engineering Aspects.

[7] Bhushan, B. , & Yong, C. J. . micro-and nanoscale characterization of hydrophobic and hydrophilic leaf surfaces institute of physics publishing micro-and nanoscale characterization of hydrophobic and hydrophilic leaf surfaces.

[8] Teisala, Hannu, Mikko Tuominen, and Jurkka Kuusipalo. "Adhesion mechanism of water droplets on hierarchically rough superhydrophobic rose petal surface." Journal of Nanomaterials 2011 (2011).

[9] Webb HK,et al, Wettability of natural superhydrophobic surfaces,Adv Colloid interface Sci(2014), http//dx.doi.org/10.1016/j.cis.2014.01.020

[10] Chakraborty, M., Weibel, J. A., Schaber, J. A., & Garimella, S. V. (2019). The wetting state of water on a rose petal. Advanced Materials Interfaces, 6(17), 1900652.

[11] Su, Yewang, et al. "Nature's design of hierarchical superhydrophobic surfaces of a water strider for low adhesion and low-energy dissipation." Langmuir 26.24 (2010): 18926-18937.

[12] Schmuser, L., Zhang, W., Marx, M. T., Encias, N., Vollmer, D., Gorb, S., ... & Weidner, T. (2020). Role of surface chemistry in the superhydrophobicity of the springtail orchesella cinta

(Insecta: Collembola). ACS applied materials & interfaces, 12(10), 12294-12304
[13] Kang, S. M., & choi, J. S. (2020). Selective Liquid Sliding Surfaces with Springtail-Inspired Concave Mushroom-Like Micropillar Arrays. Small, 16(3), 1904612.
[14] Sun, G. , Fang, Y. , Qian, C. , & Ren, L. Q. . (2009). Anisotropism of the non-smooth surface of butterfly wing. Journal of bionic engineering: Ehglish version, (1), 6.
[15] Jiang, X. , Shi, T. L. , Zuo, H. B. , Yang, X. F. , Wenjun, W. U. , & Liao, G. L. . (2012). Investigation on color variation of morpho butterfly wings hierarchical structure based on pca. Science China: Technological science ehglish version, 55(1), 6.
[16] Steve. H .(2002). The wing of a butterfly. Global CosmInd, 170(8), 32-35
[17] Yan, F. , Gang, S. , Tong-Qing, W. , Qian, C. , & Lu-Quan, R. . (2007). Effect of non-smooth scale on surface wettability of butterfly wings. Journal of Jilin University(Engineering and Technology Edition).
[18] Yan, F. , Gang, S. , Tong-Qing, W. , Qian, C. , & Lu-Quan, R. . (2007). Hydrophobicity mechnism of non-smooth pattern on surface of butterfly wing. Chinese Science Bulletin, 52(5), 711-716
[19] Bhushan, D. B. . (2010). Shark-skin surfaces for fluid-drag reduction in turbulent flow: a review. Philos Trans A Math Phys Eng, 368(1929), 4775-4806.
[20] Reif, W. E. , & Dinkelacker, A. . (1982). Hydrodynamics of the squamation in fast swimming sharks. Neues Jahrbuch für Geologie und Paläontologie - Abhandlungen, 164(1-2), 184-187.
[21] Reif, W. E. . (1985). Squamation and ecology of sharks. Courier Forschungsinstitut Senckenberg Nr. 78, pp 1-255, Frankfurt am Main.
[22] Bechert, D. W. , Bruse, M. , Hage, W. , Hoeven, J. , & Hoppe, G. . (1997). Experiments on drag-reducing surfaces and their optimization with an adjustable geometry. Journal of Fluid Mechanics, 338(1997), 59-87.
[23] Kline, S. J. , Reynolds, W. C. , Schraub, F. A. , & Runstadler, P. W. . (1967). The structure of turbulent boundary layers. Journal of Fluid Mechanics Digital Archive, 30(4), 741-0.
[24] Lee, S. J. , & Lee, S. H. . (2001). Flow field analysis of a turbulent boundary layer over a riblet surface. Experiments in Fluids, 30(2), 153-166.
[25] Hoyt, J. W. . (1975). Hydrodynamic drag reduction due to fish slimes. Swimming and Flying in Nature 2, 653–672.
[26] Shephard, K. L. .(1994). Functions for fish mucus. Rev. Fish Biol. Fish. 4, 401–429.
[27] Watson, G. S. , Green, D. W. , Schwarzkopf, L. , Li, X. , Cribb, B. W. , & Myhra, S. , et al. (2015). A gecko skin micro/nano structure – a low adhesion, superhydrophobic, anti-wetting, self-cleaning, biocompatible, antibacterial surface. Acta Biomaterialia, 21, 109-122.
[28] Spinner M. , Gorb, S. N. ,& Westhoff, G. . (2013). Diversity of functional microornamentation in slithering geckos Lialis (Pygopodidae). Proc R Soc B 2013;280:20132160.
[29] Mader, D. R. . (2006). Reptile medicine and surgery.
[30] Luisa, Dalla, Valle, Alessia, Nardi, & Vania, et al. (2007). Cloning and characterization of scale β-keratins in the differentiating epidermis of geckoes show they are glycine-proline-serine–rich proteins with a central motif homologous to avian β-keratins. Developmental Dynamics.
[31] Toni, M. , Valle, L. D. , & Alibardi, L. . (2007). The epidermis of scales in gecko lizards contains multiple forms of β-keratins including basic glycine-proline-serine-rich proteins. Journal of Proteome Research, 6(5), 1792-1805.
[32] Vazirinasab, E., Jafari, R., Momen, G., & Carreira, T. (2018). Simple fabrication of superhydrophobic surfaces using atmospheric-pressure plasma. In Materials Science Forum (Vol. 941, pp. 1808-1814). Trans Tech Publications Ltd.
[33] Zhang, Y., Zhang, Z., Yang, J., Yue, Y., & Zhang, H. (2022). Fabrication of superhydrophobic surface on stainless steel by two-step chemical etching. Chemical Physics Letters, 797, 139567.
[34] Satyarathi, J., Kumar, V., Kango, S., Sharma, N., & Verma, R. (2022, July). Fabrication of Superhydrophobic Surface on Low Carbon Steel. In IOP Conference Series: Materials Science and Engineering (Vol. 1248, No. 1, p. 012015). IOP Publishing. [6.4.1] Janjua, Z. A., Turnbull, B., Hibberd, S., & Choi, K. S. (2018). Mixed ice accretion on aircraft wings. Physics of Fluids, 30(2), 027101.

[35] Janjua, Z. A., Turnbull, B., Hibberd, S., & Choi, K. S. (2018). Mixed ice accretion on aircraft wings. Physics of Fluids, 30(2), 027101.
[36] Ma, Q., Tong, Z., Wang, W., & Dong, G. (2018). Fabricating robust and repairable superhydrophobic surface on carbon steel by nanosecond laser texturing for corrosion protection. Applied Surface Science, 455, 748-757.
[37] Vanithakumari, S. C., Kumar, C. A., Thinaharan, C., Kishor, G. R., George, R. P., Kaul, R., ... & John, P. (2021). Laser patterned titanium surfaces with superior antibiofouling, superhydrophobicity, self-cleaning and durability: Role of line spacing. Surface and Coatings Technology, 418, 127257.
[38] Latthe, S. S., Sutar, R. S., Bhosale, A. K., Nagappan, S., Ha, C. S., Sadasivuni, K. K., ... & Xing, R. (2019). Recent developments in air-trapped superhydrophobic and liquid-infused slippery surfaces for anti-icing application. Progress in Organic Coatings, 137, 105373.
[39] Tran, N. G., & Chun, D. M. (2022). Ultrafast and Eco-Friendly Fabrication Process for Robust, Repairable Superhydrophobic Metallic Surfaces with Tunable Water Adhesion. ACS Applied Materials & Interfaces, 14(24), 28348-28358.
[40] Nyankson, E., Agbe, H., Takyi, G. K. S., Bensah, Y. D., & Sarkar, D. K. (2022). Recent advances in nanostructured superhydrophobic surfaces: fabrication and long-term durability challenges. Current Opinion in Chemical Engineering, 36, 100790.
[41] Mirzadeh, M., Dehghani, K., Rezaei, M., & Mahidashti, Z. (2019). Effect of stearic acid as a low cost and green material on the self-cleaning and anti-corrosion behavior of anodized titanium. Colloids and Surfaces A: Physicochemical and Engineering Aspects, 583, 123971.
[42] Manoj, T. P., Rasitha, T. P., Vanithakumari, S. C., Anandkumar, B., George, R. P., & Philip, J. (2020). A simple, rapid and single step method for fabricating superhydrophobic titanium surfaces with improved water bouncing and self cleaning properties. Applied Surface Science, 512, 145636.
[43] Shen, Y., Wu, X., Tao, J., Zhu, C., Lai, Y., & Chen, Z. (2019). Icephobic materials: Fundamentals, performance evaluation, and applications. Progress in Materials Science, 103, 509-557.
[44] Jeevahan, J., Chandrasekaran, M., Britto Joseph, G., Durairaj, R. B., & Mageshwaran, G. J. J. O. C. T. (2018). Superhydrophobic surfaces: a review on fundamentals, applications, and challenges. Journal of Coatings Technology and Research, 15(2), 231-250.
[45] Hwang, G. B., Page, K., Patir, A., Nair, S. P., Allan, E., & Parkin, I. P. (2018). The anti-biofouling properties of superhydrophobic surfaces are short-lived. ACS nano, 12(6), 6050-6058.
[46] Zhang, B., & Xu, W. (2021). Superhydrophobic, superamphiphobic and SLIPS materials as anti-corrosion and anti-biofouling barriers. New Journal of Chemistry.
[47] Shang, Q., & Zhou, Y. (2016). Fabrication of transparent superhydrophobic porous silica coating for self-cleaning and anti-fogging. Ceramics International, 42(7), 8706-8712.
[48] Ma, M., Hill, R. M., & Rutledge, G. C. (2008). A review of recent results on superhydrophobic materials based on micro-and nanofibers. Journal of Adhesion Science and Technology, 22(15), 1799-1817.
[49] Nakajima, A., Hashimoto, K., & Watanabe, T. (2001). Recent studies on super-hydrophobic films. Molecular Materials and Functional Polymers, 31-41.
[50] Bocquet, L., & Lauga, E. (2011). A smooth future?. Nature materials, 10(5), 334-337.